Published in *Proceedings of the IGARSS - IEEE International Geoscience and Remote Sensing Symposium 2022,* Kuala Lumpur, Malaysia , 17-22 July 2022, which should be cited to refer to this work.
DOI: 10.1109/IGARSS46834.2022.9883336

A GPS MOVING BASELINE NAVIGATION SYSTEM ON A SAR DRONE TESTED IN AN EXPERIMENT TO ANALYZE THE SIGNATURE OF COVERED REFLECTORS

Peter Brotzer, Daniel Henke

University of Zurich, RSL, Switzerland

Sébastien Guillaume

HEIG-VD, INSIT, Switzerland

ABSTRACT

The miniaturization of frequency-modulated continuous-wave synthetic aperture radar systems has become increasingly important in recent years. In this paper, we present the ongoing improvements on our SAR drone hardware setup, with special focus on the integration of moving baseline aided navigation data. Furthermore, an experiment investigates the detection of covered reflectors, determines the attenuation factor, and demonstrates the advantages of moving baseline supported processing.

Index Terms— Synthetic Aperture Radar, SAR, FMCW, UAV, Drone, Moving Baseline

1. INTRODUCTION

The development of frequency-modulated continuous wave (FMCW) synthetic aperture radar (SAR) allows the main components to be miniaturized. The reduction in weight, as well as affordability of purchase, makes it possible to install SAR systems on drones. These factors are driving an increase in the prevalence of drone-based SAR systems in academic research. However, miniaturization also comes with drawbacks. Especially by requirement of weight limitation, trade-offs have to be made affecting SAR image quality. High-precision IMUs are often too heavy or costly to integrate into drone systems. Software-based solutions for focusing are therefore widely used, although its applicability often depends on the characteristics of the specific scene [1].

Even though drone SAR is still an emerging topic at the moment, several groups proposed setups and demonstrated applications [2, 3, 4, 5]. A high-resolution low-cost drone-borne SAR imaging system at 77 GHz and 1 GHz bandwidth was proposed without using inertial navigation system (INS) or Global Positioning System (GPS) [2]. For a SAR-scene, recorded with a flight altitude of 20 m, a resolution of below 5 cm in range and cross-range was demonstrated. Likewise, even the possibility of combining C-band L-band and P-band on a drone for crop growth monitoring was presented [3].

SAR-drone systems are interesting for detection of various objects because of their flexibility. The theoretical design of an ultra high frequency ultra wide band for detection of buried objects like landmines is shown in [4]. In low-altitude experiments the capability of the detection of three different types of mines was investigated. Detection of hidden persons in a forest for search and rescue SAR mission was presented in [5]. Using predefined flight paths, a high percentage of people were able to be found, which can be increased with adaptive flight planning.

In this paper, in a basic experiment the detection of two differently covered corner reflectors is presented while demonstrating the advantages of a RTK GPS positioning and moving baseline system. It is analyzed whether a corresponding reflected intensity attenuation value can be attributed to the chosen materials. The coverage used were bark mulch and tree branches. Since our sensor operates in C-band we are limited to light coverage materials that resemble forest canopies with different densities, which we intend to simulate with the above materials. In experiments under controllable conditions, the attenuation factors are determined with respect to uncovered reflectors. An Ancortek FMCW radar operating at 5.8 GHz with 400 MHz bandwidth is utilized for acquiring data.

Because the functionality of commercially available components is not optimized for SAR applications, their weaknesses are discussed and improvements to these components are presented. A radar system based on a hardware-modified, improved version of the so-called Radarbook [6], operating in K-band at 24 GHz and 700 MHz bandwidth, is intended to overcome certain limitations. A special focus is on controlling the parameters and increasing the transmission power to enable SAR acquisitions from a larger distance. Also, it was observed in the experiment that the internal navigation data of the drone (obtained by combining GNSS and low-cost INS) is not sufficient to achieve optimal image quality. Therefore, it is demonstrated why the integration of a moving baseline setup can be advantageous. The performance against commercially provided navigation data is examined.

The paper is structured in the following way: In Section 2 the experimental setup is introduced as well as specifications of the sensors. The moving baseline method is presented in Section 3. The results of the experiment with the covered reflectors are shown in Section 4. In addition, the comparison between the merged moving baseline and the DJI navigation SAR-image are presented. Section 5 summarizes previous results and suggests potential future investigations.

Parameter	Ancortek	Radarbook
Carrier frequency	5.8 GHz	24 GHz
Bandwidth	400 MHz	700 MHz
PRF	1 kHz	1 kHz
Transmission power	21 dBm	up to 30 dBm
Depression angle	45 °	30 °

Table 1. System parameters

2. EXPERIMENTAL SETUP

2.1. Hardware

2.1.1. Radar

The Ancortek radar system with patch antennas used in the experiment operates in C-band at a frequency of 5.8 GHz and a bandwidth of 400 MHz. Additional properties can be found in Table 1. Due to its limited transmission power, the radar is only suitable for data acquisition at low-altitude flight, typically below 30 m. The range and azimuth resolution are 0.37 m and 0.06 m, respectively.

Because of the limitations of the Ancortek radar, we are working to improve the SAR system by replacing the current radar with a modified Radarbook sensor. It operates in K-band with a frequency of 24 GHz and a bandwidth of 700 MHz. This results in a range and azimuth resolution of 0.21 m and 0.04 m, respectively. In the Radarbook, the output signal was decoupled from the signal generator, connected to an external power amplifier, and then routed to the horn antenna to increase the transmission power by the desired amount. This is done to improve the maximum range of the radar system. However, the higher frequency of the system could counteract the increase a bit. Data were recently acquired with the new K-Band system on the drone platform. Preliminary images have been focused. The detailed analysis and fine-tuning are currently being carried out, so we expect to be able to show first results during the presentation at the conference.

2.1.2. Navigation

The navigation data for the SAR processing of the first part of the experiment we obtain from the DJI A2 Flight Control System. It obtains the GPS information from the three DJI GPS-Compass Pro Plus receivers on top of the drone. These data are internally merged together with the data from the two DJI IMU Pro modules by using a Kalman filter.

Low-cost INS often have the disadvantage that over time drift causes inaccurate position and attitude data. This problem can be intrinsically fixed by using a moving baseline. Figure 1 shows the moving baseline on our drone consisting of

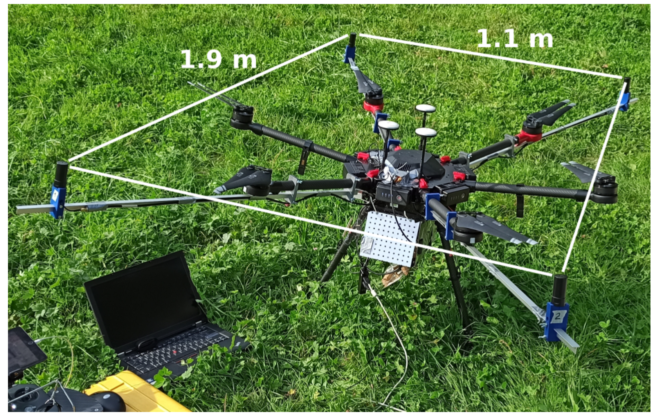

Fig. 1. C-band SAR drone platform with highlighted moving baseline

four GNSS AS-ANT2B-HEL-L1L2-SMA-00 helix active antennas mounted on extensions of the drone arms. The geometry of the antennas is formed by a quasi-rectangle pattern of approximatively 1×2 m. In addition, a Xsens INS is placed on top of the drone for data fusion with the moving baseline data.

2.2. Data acquisition

The setup of the experiment can be seen in Figure 2. Three reference reflectors of equal size were placed in a row, parallel to the flight path of the drone to avoid an influence of the antenna pattern (Figure 2 (d)). In a first reference flight, the signatures of the uncovered reflectors were recorded. After covering one reflector with bark mulch and an other one with tree branches the signatures were recorded in several flights.

3. MOVING BASELINE METHOD

The GNSS moving baseline technique is able to provide the attitude without long-term drift, but with a sampling rate of 2 Hz in both frequencies L1+L2 and a noise of about 1° for a baseline more than 1 m. Moreover, the quality of the attitude obtained by this technique depends strongly on the external environment and the available visible satellites. In contrast, the attitude obtained by the integration of angular velocities provided by gyroscopes suffers drifts and random walks, but are able to provide high-rate data, of several hundred Hertz. This involves that long term precision of gyroscopes attitudes is low. However, the relative precision of gyroscopes attitudes can be high ($< 0.1°$) for short time differences. In addition, the quality of the data provided by the gyroscopes is more constant, and much less influenced by external conditions. In this context, the fusion of both techniques using a Kalman filter based approach should improve the accuracy of the attitude in a large scope and enhance the continuity and

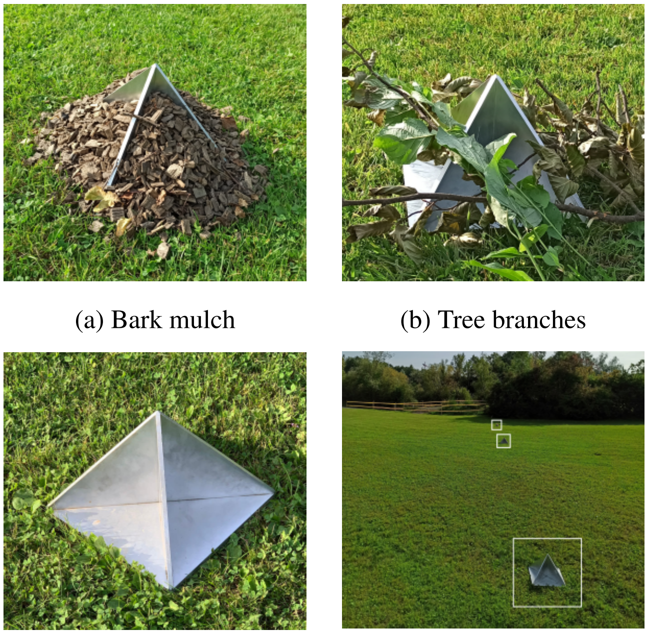

(a) Bark mulch (b) Tree branches

(c) Uncovered (d) Scenery

Fig. 2. Experimental setup: the three corner reflector can either be covered with bark mulch, tree branches or uncovered.

the robustness of the attitude determination.

Prior to the experiment, it was ensured that in this configuration, the GNSS signals are not affected by the propellers and the radar. Fixed ambiguities solutions are almost always available when the drone is in a normal flying mode. The Kalman filter solution, at 100 Hz, combining GNSS attitude angles with angular velocities from a 3-axis gyroscope, performs with an accuracy better than 0.1°. The initialization of the Kalman filter needs approximately 1 minute.

4. RESULTS AND EVALUATION

The results from the two drone flights at altitude of 25 m are shown in Figure 3. In the left image, the three bright points correspond to the uncovered corner reflectors from the reference flight. All reflectors appear approximately equally bright in the image with less than 6% deviation from their mean amplitude value. The large signature below the reflectors originates from the nearby bush. Figure 3 (b) shows the same scene but with the signature of covered reflectors. The top reflector is uncovered, the one below is covered with bark mulch and the bottom one is covered with tree branches resulting in attenuation factors of 8.29 ± 0.32 dB and 5.98 ± 0.51 dB, respectively.

Processing the SAR image of a flight once with the merged moving baseline navigation data and once with the DJI navigation data, the difference can be seen in Figure 4.

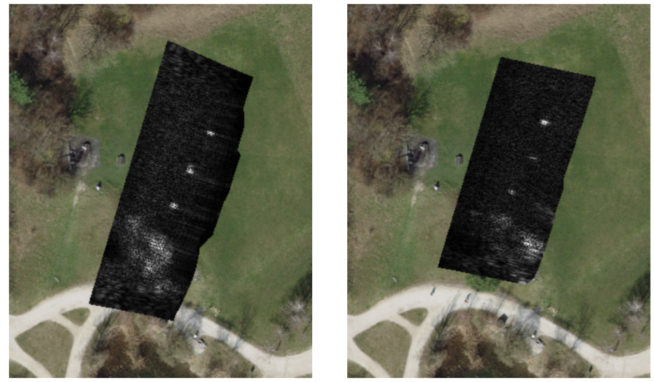

(a) Reference flight (b) Experimental flight

Fig. 3. SAR images of test flights overlayed on optical image. In (a) the result the reference flight is shown. The signature of the covered reflectors is presented in (b).

The reflectors focused by the RTK GPS positioning moving baseline navigation data merged with the Xsens IMU data are brighter in the image than the reflectors focused by the DJI navigation data. Comparing the 5 brightest pixels of each reflector signature to the corresponding other one, an averaged 1.93 ± 0.31 dB higher reflected intensity is measured. Analyzing the signature of the reflectors in Figure 4 (a), a ground range resolution of $\delta r_{gr} = 0.98$ m and azimuth resolution of $\delta az = 0.1$ m is determined. For the SAR image in Figure 4 (b), a resolution of $\delta r_{gr} = 1.1$ m, $\delta az = 0.23$ m is observed. Comparing both to the theoretical resolution of $\delta r_{gr} = 0.53$ m, $\delta az = 0.06$ m, it can be seen that with the merged moving baseline navigation data, a considerable improvement in the azimuth resolution is achieved. It has been expected that better navigation data does not necessarily translate into better resolution in range. Defocusing resulting from inaccurate localization primarily affects the azimuth direction. The non-optimal focusing in range might be caused by a problem on the radar system side. This is currently resolved by replacing the current radar with its successor.

In addition, Figure 4 (c) shows an example of how the pure GNSS based yaw data is enhanced by the Xsens IMU data. The yaw values, which come from the 2 Hz moving baseline data, are merged with the 100 Hz INS data through a Kalman filter. Especially in the case of rapid changes, one benefits from the additional information of the IMU. A purely GPS-based determination of position and attitude does not meet the requirements for drone SAR. Looking at the pure INS yaw data, a slight drift over time is observed. Relying only on gyroscope measurements of attitude data would result in a loss of quality.

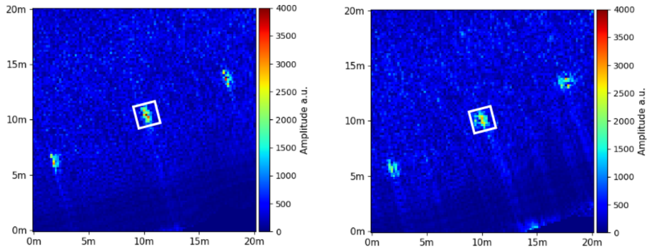

(a) Merged moving baseline (b) DJI

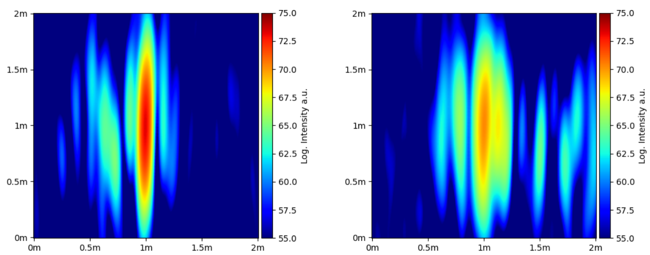

(c) MB, reflector 2 (d) DJI, reflector 2

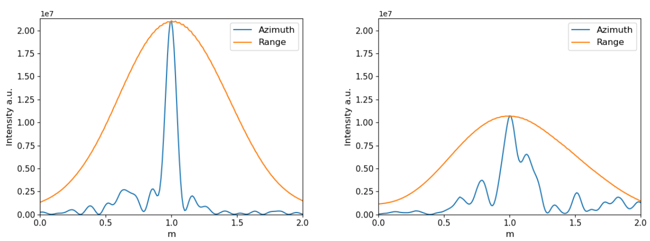

(e) MB, resolution (f) DJI, resolution

Fig. 4. Experimental evaluation of moving baseline system. SAR-image processed with merged moving baseline data and with DJI navigation data.

5. CONCLUSION & OUTLOOK

In this paper, we presented a drone setup, which is equipped with a moving baseline system. The experiment demonstrated the advantages of moving baseline navigation data compared to commercial low-cost INS systems. An overall better focusing of the SAR-image is achieved (1.93 ± 0.31 dB). Furthermore, in the experiments, limited to light coverage cases, the materials bark mulch and tree branches have been assigned an attenuation factor of 8.29 ± 0.32 dB and 5.98 ± 0.51 dB, respectively. This experiment is to be repeated with the newly equipped radar system by the time of the conference. In particular, the new radar is intended to achieve a higher signal-to-noise ratio and enable higher flight altitudes.

As the trend is not only towards high-resolution radar systems but also towards low-cost systems, the integration of moving baselines into SAR systems should be further investigated. Precise attitude data can be critical to perform radiometric calibration.

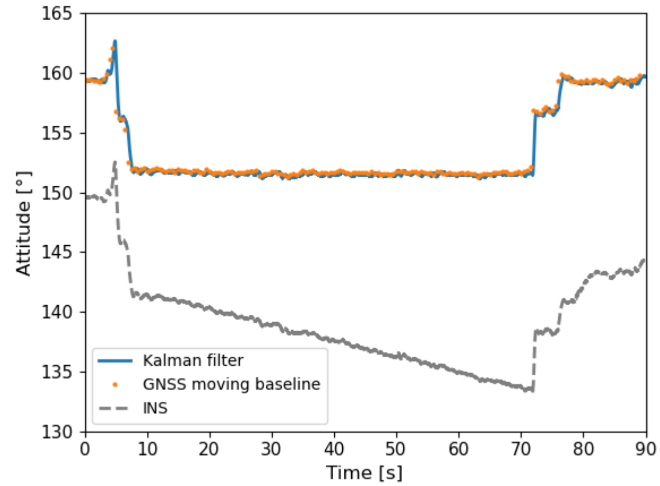

Fig. 5. Merging of GNSS only moving baseline yaw data with gyroscopic Xsens INS measurements.

6. REFERENCES

[1] Marc Lort, Albert Aguasca, Carlos Lopez-Martinez, and Tomás Martínez Marín, "Initial evaluation of SAR capabilities in UAV multicopter platforms," *IEEE Journal of Selected Topics in Applied Earth Observations and Remote Sensing*, vol. 11, no. 1, pp. 127–140, 2017.

[2] Ali Bekar, Michail Antoniou, and Christopher J Baker, "Low-cost, high-resolution, drone-borne SAR imaging," *IEEE Transactions on Geoscience and Remote Sensing*, 2021.

[3] Gian Oré, Marlon S. Alcântara, Juliana A. Góes, Luciano P. Oliveira, Jhonnatan Yepes, Bárbara Teruel, Valquíria Castro, Leonardo S. Bins, Felicio Castro, Dieter Luebeck, et al., "Crop growth monitoring with drone-borne DInSAR," *Remote Sensing*, vol. 12, no. 4, pp. 615, 2020.

[4] Marius Engel, Andreas Heinzel, Eric Schreiber, Stephan Dill, and Markus Peichl, "Recent results of a UAV-based synthetic aperture radar for remote sensing applications," in *EUSAR; 13th European Conference on Synthetic Aperture Radar*. VDE, 2021, pp. 1–5.

[5] David C Schedl, Indrajit Kurmi, and Oliver Bimber, "An autonomous drone for search and rescue in forests using airborne optical sectioning," *Science Robotics*, vol. 6, no. 55, 2021.

[6] INRAS, "Radarbook2," 2022, https://inras.at/en/radarbook2/ [Online; accessed 15-January-2022].